

The influence of strength of hyperon-hyperon interactions on neutron star properties.

I. Bednarek and R. Manka §

Department of Astrophysics and Cosmology, Institute of Physics, University of Silesia, Uniwersytecka 4, PL-40-007 Katowice, Poland

Abstract. An equation of state of neutron star matter with strange baryons has been obtained. The effects of the strength of hyperon-hyperon interactions on the equations of state constructed for the chosen parameter sets have been analyzed. Numerous neutron star models show that the appearance of hyperons is connected with the increasing density in neutron star interiors. The performed calculations have indicated that the change of the hyperon-hyperon coupling constants affects the chemical composition of a neutron star. The obtained numerical hyperon star models exclude large population of strange baryons in the star interior.

1. Introduction

The analysis of the role of strangeness in nuclear structure in the aspect of multi-strange system is of great importance for relativistic heavy-ion collisions and for astrophysics for the description of hyperon star matter. At the core of a neutron star the matter density ranges from a few times the density of normal nuclear matter to about an order of a magnitude higher. Thus exotic forms of matter such as hyperons are expected to emerge in the interior of a neutron star. The appearance of these additional degrees of freedom and their impact on a neutron star structure have been the subject of extensive studies [1], [2], [3], [4]. Properties of matter at such extreme densities are of particular importance in determining forms of equations of state relevant to neutron stars and successively in examining their global parameters.

The existence of bound strange hadronic matter which in addition to nucleons contains also hyperons has profound consequences for astrophysics. The starting point in studying the role of strangeness in nuclear structure is the knowledge of the properties of a single hypernucleus. Quantum chromodynamics should be applied to the theoretical description of hadronic systems owing to the fact that it constitutes the fundamental theory of strong interactions. However, at the hadronic energy scale where the experimentally observed degrees of freedom are not quarks but hadrons the direct description of nuclei in terms of QCD become inadequate and thus alternative approaches had to be formulated. One of them is quantum hadrodynamics (QHD) [5], [6] which gives quantitative description of the nuclear many body problem. QHD is a relativistic quantum field theory in which nuclear matter description in terms of baryons and mesons is provided. The original model (QHD-I) contains nucleons interacting through the exchange of simulating medium range attraction σ meson and ω meson responsible for short range repulsion. Extension (QHD-II) of this theory [7],[8] includes also the isovector meson ρ . Theoretical description of strange hadronic matter, which satisfactorily reproduces nucleon-nucleon and hyperon-nucleon data, has been given within the non-relativistic and relativistic mean field models. This approach is based on the notion of the meson-exchange model in which baryons interact through the exchange of mesons. In addition to the σ , ω and ρ mesons these models contain σ^* and ϕ mesons, introduced in order to reproduce the strong attractive hyperon-hyperon interactions [9]. The vector coupling constants are chosen according to SU(6) symmetry whereas the scalar coupling constants are fixed to hypernuclear data. Recent reports on observations of a ${}^6_{\Lambda\Lambda}He$ hypernucleus made by Takahashi et al. [10] provided information on the $\Lambda - \Lambda$ interaction energy $\delta B_{\Lambda\Lambda} = 1.01 \pm 0.20^{+0.18}_{-0.11}$ MeV. This allows one to determine the value of the Λ well depth in Λ matter at density $0.5\rho_0$ (ρ_0 denotes the saturation density) at the level of $U_{\Lambda}^{\Lambda} \simeq 5$ MeV [11]. The results of earlier experiments [12], [13], [14], [15], [16] give the value of U_{Λ}^{Λ} estimated with the use of Nijmegen model D at the level of $\simeq 20$ MeV [9]. This paper examines the implications of the strength of hyperon-hyperon coupling constants on the β -equilibrated hyperon star matter, hence doing all calculations within the framework of relativistic mean field model with two

parameterizations, namely the standard TM1 [17] and TMA [18]. The results have been obtained for two cases: the weak and strong $Y - Y$ interactions. First, the properties of the isospin symmetric strange hadronic matter have been investigated. The obtained saturation curves resemble those obtained by Song et al.[11]. The results for the two models (TM1 and TMA) are very similar. The extension of the considered model to the β equilibrated asymmetric hyperon star model has been done in the subsequent section. As a result of this the composition, the equation of state and the hyperon star structure for the two parameterizations have been obtained.

2. Hypernuclei

Information on single hypernuclei can be summarized in the following points:

- Λ hypernuclei: there is a large amount of data on the binding energies B_Λ of Λ 's bound in various single particle orbitals in hypernuclei. This enables us to study deeply bound states inside the nucleus over an extensive range of mass number. An analysis of these data with the use of Skyrme-Hartree-Fock [19] model gives the potential depth of a single Λ in nuclear matter at the value of

$$U_\Lambda^{(N)} \simeq 27 - 30 \text{ MeV} \quad (1)$$

which corresponds to 1/3-1/2 of the nucleon well depth $U_N^{(N)}$ (in this text all potentials are considered as attractive but the convention of positive sign has been used).

- Σ hypernuclei [20]: the experimental status of Σ nucleus potential still remains controversial. The calculations of Σ hypernuclei have been based on analysis of Σ^- atomic data. Phenomenological analysis of level shifts and widths in Σ^- atoms made by Batty et al. [21] indicates that the Σ potential is attractive only at the nuclear surface changing into repulsive one in increasing density. The small attractive component of this potential is not sufficient to form bound Σ -hypernuclei. Balberg et al. in their paper [22] show that the system which includes Σ , Λ hyperons and nucleons will be unstable with respect to strong reactions $\Sigma + N \rightarrow \Lambda + N$ (78 MeV), $\Sigma + \Sigma \rightarrow \Lambda + \Lambda$ (156 MeV), $\Sigma + \Lambda \rightarrow \Xi + N$ (50 MeV), $\Sigma + \Xi \rightarrow \Lambda + \Xi$ (80 MeV) [23], in parenthesis the Q values for each reaction are given.
- Ξ hypernuclei - for the Ξ hypernuclei there exist a few emulsion events reported in literature indicating the existence of a bound system. The interpreted data give the potential of a Ξ in nuclear matter with a depth of

$$U_\Xi^{(N)} \simeq 20 - 25 \quad \text{MeV}. \quad (2)$$

- $\Lambda\Lambda$ hypernuclei: the properties of single hypernuclei are one aspect of studying strangeness in nuclear systems; the other is connected with multi-strange systems. The extrapolation to a multi-strange system is based on the data concerning double Λ -hypernuclei. Data on $\Lambda\Lambda$ hypernuclei are extremely scarce. Observation of double-strange hypernuclei $\Lambda\Lambda$ provide information about the $\Lambda - \Lambda$ interaction.

Hypernucleus	$B_{\Lambda\Lambda}[\text{MeV}]$	$\Delta B_{\Lambda\Lambda}[\text{MeV}]$
${}^6_{\Lambda\Lambda}\text{He}$	10.9 ± 0.6	4.7 ± 0.6
${}^{10}_{\Lambda\Lambda}\text{Be}$	17.7 ± 0.4	4.3 ± 0.4
${}^{13}_{\Lambda\Lambda}\text{B}$	27.5 ± 0.7	4.8 ± 0.7

Table 1. The value of $\Delta B_{\Lambda\Lambda}$ and $B_{\Lambda\Lambda}$ of the known double Λ -hypernuclei.

Several events have been identified which indicate an attractive $\Lambda\Lambda$ interaction. The analysis of the data allows one to estimate the binding energies of ${}^6_{\Lambda\Lambda}\text{He}$, ${}^{10}_{\Lambda\Lambda}\text{Be}$ and ${}^{13}_{\Lambda\Lambda}\text{B}$. The measurement of the masses of double- Λ hypernuclei gives information on the sum of the binding energy of the two Λ hyperons $B_{\Lambda\Lambda}$ and the $\Lambda - \Lambda$ interaction energy $\Delta B_{\Lambda\Lambda}$. These two quantities can be defined as

$$\begin{aligned} B_{\Lambda\Lambda}({}^A_{\Lambda\Lambda}Z) &= B_{\Lambda}({}^A_{\Lambda\Lambda}Z) + B_{\Lambda}({}^{A-1}_{\Lambda}Z) \\ \Delta B_{\Lambda\Lambda}({}^A_{\Lambda\Lambda}Z) &= B_{\Lambda}({}^A_{\Lambda\Lambda}Z) - B_{\Lambda}({}^{A-1}_{\Lambda}Z). \end{aligned} \quad (3)$$

Table 2 compiles experimental values of the two observables mentioned above [13], [15], [14], [12]. The obtained values of $\Delta B_{\Lambda\Lambda}$ indicate that the $\Lambda - \Lambda$ interaction is attractive and rather strong. The value of ΔB_{NN} equals 6-7 MeV for comparison. Following the estimation made by Schaffner et al.[9] it is possible to approximately determine the ratio of the Λ well depth in Λ matter and nucleon well depth in nuclear matter

$$\frac{U_{\Lambda}^{(\Lambda)}}{U_N^{(N)}} = \frac{V_{\Lambda\Lambda}}{V_{NN}} \frac{1/4}{3/8} \quad (4)$$

where $1/2$ stands for a nucleon and Λ density ratio and $(1/4)/(3/8)$ denotes spin-isospin weights of spatially symmetric two-body configurations. Taking into account the value of $V_{\Lambda\Lambda} \equiv \Delta B_{\Lambda\Lambda} \simeq 4 - 5$ MeV and the value $V_{NN} \simeq 6 - 7$ MeV one can estimate the ratio $V_{\Lambda\Lambda}/V_{NN} \approx 3/4$ and thus the equation (4) gives

$$\frac{U_{\Lambda}^{(\Lambda)}}{U_N^{(N)}} \approx \frac{1}{4}. \quad (5)$$

For $U_N^N \simeq 80$ MeV the estimated value of U_{Λ}^{Λ} potential is $\simeq 20$ MeV.

However, the recent data analysis of double hypernucleus ${}^6_{\Lambda\Lambda}\text{He}$ done by Takahashi et al. [10] gives the following value of the $\Lambda - \Lambda$ interaction energy $\Delta B_{\Lambda\Lambda} = 1.01 \pm 0.20^{+0.18}_{-0.11}$ MeV what indicate that the interaction is much weaker. The potential well depth evaluated for this data has the value $U_{\Lambda}^{(\Lambda)} \simeq 5$ MeV.

3. The model

The theoretical description of the properties of strange hadronic matter is given within the relativistic mean field approach. The considered model involves baryons interacting

through the exchange of simulating medium range attraction σ meson and ω meson responsible for short range repulsion. The model also includes the isovector meson ρ . In order to reproduce attractive hyperon-hyperon interaction two additional hidden-strangeness mesons, which do not couple to nucleons, have been introduced, namely the scalar meson $f_0(975)$ (denoted as σ^*) and the vector meson $\phi(1020)$.

The effective Lagrangian function for the system can be written as a sum of a baryonic part including the full octet of baryons together with baryon-meson interaction terms and a mesonic part

$$\mathcal{L} = \mathcal{L}_B + \mathcal{L}_M. \quad (6)$$

The interacting baryons are described by the Lagrangian function \mathcal{L}_B which is given by

$$\mathcal{L}_B = \sum_B \bar{\psi}_B (i\gamma^\mu D_\mu - m_B + g_{\sigma B}\sigma + g_{\sigma^* B}\sigma^*)\psi_B. \quad (7)$$

where B stands for N, Λ, Σ, Ξ and $\Psi_B^T = (\psi_N, \psi_\Lambda, \psi_\Sigma, \psi_\Xi)$. The covariant derivative D_μ is defined as

$$D_\mu = \partial_\mu + ig_{\omega B}\omega_\mu + ig_{\phi B}\phi_\mu + ig_{\rho B}I_{3B}\tau^a\rho_\mu^a. \quad (8)$$

The Lagrangian density for meson fields takes the form

$$\begin{aligned} \mathcal{L}_M = & \frac{1}{2}\partial_\mu\sigma\partial^\mu\sigma - U(\sigma) + \frac{1}{2}\partial_\mu\sigma^*\partial^\mu\sigma^* - \frac{1}{2}m_{\sigma^*}^2\sigma^{*2} + \\ & + \frac{1}{2}m_\phi^2\phi_\mu\phi^\mu - \frac{1}{4}\phi_{\mu\nu}\phi^{\mu\nu} - \frac{1}{4}\Omega_{\mu\nu}\Omega^{\mu\nu} + \frac{1}{2}m_\omega^2\omega_\mu\omega^\mu + \\ & - \frac{1}{4}R_{\mu\nu}^a R^{a\mu\nu} + \frac{1}{2}m_\rho^2\rho_\mu^a\rho^{a\mu} + \frac{1}{4}c_3(\omega_\mu\omega^\mu)^2. \end{aligned} \quad (9)$$

The field tensors $R_{\mu\nu}^a, \Omega_{\mu\nu}, \phi_{\mu\nu}$ are defined as

$$R_{\mu\nu}^a = \partial_\mu\rho_\nu^a - \partial_\nu\rho_\mu^a + g_\rho\varepsilon_{abc}\rho_\mu^b\rho_\nu^c, \quad (10)$$

$$\Omega_{\mu\nu} = \partial_\mu\omega_\nu - \partial_\nu\omega_\mu, \quad \phi_{\mu\nu} = \partial_\mu\phi_\nu - \partial_\nu\phi_\mu \quad (11)$$

The potential function $U(\sigma)$ possesses a polynomial form

$$U(\sigma) = \frac{1}{2}m_\sigma^2\sigma^2 + \frac{1}{3}g_3\sigma^3 + \frac{1}{4}g_4\sigma^4. \quad (12)$$

The baryon mass is denoted by m_B whereas m_M ($M = \sigma, \omega, \rho, \sigma^*, \phi$) are masses assigned to the meson fields. The derived equations of motion constitute a set of coupled equations which have been solved in the mean field approximation. In this approximation meson fields are separated into classical mean field values and quantum fluctuations which are not included in the ground state

$$\begin{aligned} \sigma &= \bar{\sigma} + s_0 & \sigma^* &= \bar{\sigma}^* + s_0^* \\ \phi_\mu &= \bar{\phi}_\mu + f_0\delta_{\mu 0} & \omega_\mu &= \bar{\omega}_\mu + w_0\delta_{\mu 0} & \rho_\mu^a &= \bar{\rho}_\mu^a + r_0\delta_{\mu 0}\delta^{3a} \end{aligned}$$

In the field equations the derivative terms are neglected and only time-like components of the vector mesons will survive if one assumes homogenous and isotropic infinite matter. The field equations derived from the Lagrange function at the mean field level are

$$m_\sigma^2 s_0 + g_3 s_0^2 + g_4 s_0^3 = \sum_B g_{\sigma B} m_{eff,B}^2 S(m_{eff,B}, k_{F,B}) \quad (13)$$

$$m_\omega^2 w_0 + c_3 w_0^3 = \sum_B g_{\omega B} n_B \quad (14)$$

$$m_\rho^2 r_0 = \sum_B g_{\rho B} I_{3B} n_B \quad (15)$$

$$m_{\sigma^*}^2 s_0^* = \sum_B g_{\sigma^* B} m_{eff,B}^2 S(m_{eff,B}, k_{F,B}) \quad (16)$$

$$m_\phi^2 f_0 = \sum_B g_{\phi B} n_B. \quad (17)$$

The function $S(m_{eff,B}, k_{F,B})$ is expressed with the use of the integral

$$S(m_{eff,B}, k_{F,B}) = \frac{2J_B + 1}{2\pi^2} \int_0^{k_{F,B}} \frac{m_{eff,B}}{\sqrt{k^2 + m_{eff,B}^2}} k^2 dk \quad (18)$$

where J_B and I_{3B} are the spin and isospin projections of baryon B , $k_{F,B}$ is the Fermi momentum of species B , $n_B = \gamma_B k_{F,B}^3 / 6\pi^2$ (γ_B stands for the spin-isospin degeneracy factor which equals 4 for nucleons and Ξ hyperons and 2 for Λ).

The obtained Dirac equation for baryons has the following form

$$(i\gamma^\mu \partial_\mu - m_{eff,B} - g_{\omega B} \gamma^0 \omega_0 - g_{\phi B} \gamma^0 f_0) \psi_B = 0 \quad (19)$$

with $m_{eff,B}$ being the effective baryon mass generated by the baryon and scalar fields interaction and defined as

$$m_{B,eff} = m_B - (g_{\sigma B} s_0 + g_{\sigma^* B} s_0^*). \quad (20)$$

The total energy of the system is given by

$$\begin{aligned} \varepsilon = & \frac{1}{2} m_\rho^2 r_0^2 + \frac{1}{2} m_\phi^2 f_0^2 + \frac{1}{2} m_{\sigma^*} (s_0^*)^2 + \frac{1}{2} m_\omega^2 w_0^2 \\ & + \frac{3}{4} c_3 w_0^4 + U(s_0) + \varepsilon_B \end{aligned} \quad (21)$$

where ε_B equals

$$\varepsilon_B = \sum_B \frac{1}{3\pi^2} \int_0^{k_{F,B}} k^2 dk \sqrt{k^2 + m_{eff,B}^2}. \quad (22)$$

	m_σ [MeV]	$g_{\sigma N}$	$g_{\omega N}$	$g_{\rho N}$	c_3	g_3	g_4
TM1	511.198	10.0289	12.6139	4.6322	71.3075	7.2325	0.6183
TMA	519.151	10.055	12.842	7.6	151.59	0.328	38.862

Table 2. Chosen parameter sets.

		$g_{\sigma\Lambda}$	$g_{\sigma\Xi}$	$g_{\sigma^*\Lambda}$	$g_{\sigma^*\Xi}$
TM1	weak	6.2380	3.1992	3.7257	11.5092
	strong	6.2380	3.1992	7.9429	12.5281
TMA	weak	6.2421	3.2075	4.3276	11.7314
	strong	6.2421	3.2075	8.2580	12.7335

Table 3. Strange scalar sector parameters.

4. Parameters.

The considered model does not include Σ hyperons due to the remaining uncertainty of the form of their potential in nuclear matter at saturation density [24], [21], [25]. The parameters that enter the Lagrangian function are collected in Tables 2 and 3. They are the standard TM1 parameter set [17] supplemented by hyperon-meson coupling constants. In the scalar sector the scalar coupling of the Λ and Ξ hyperons requires constraining in order to reproduce the estimated values of the potential felt by a single Λ and a single Ξ in saturated nuclear matter

$$\begin{aligned}
 U_\Lambda^{(N)}(\rho_0) &= g_{\sigma\Lambda}s_0(\rho_0) - g_{\omega\Lambda}w_0(\rho_0) \simeq 27 - 28 \text{ MeV} \\
 U_\Xi^{(N)}(\rho_0) &= g_{\sigma\Xi}s_0(\rho_0) - g_{\omega\Xi}w_0(\rho_0) \simeq 18 - 20 \text{ MeV}.
 \end{aligned}
 \tag{23}$$

Assuming the $SU(6)$ symmetry for the vector coupling constants and determining the scalar coupling constants from the potential depths, the hyperon-meson couplings can be fixed.

The strength of hyperon couplings to strange meson σ^* is restricted through the following relation

$$U_\Xi^{(\Xi)} \approx U_\Lambda^{(\Xi)} \approx 2U_\Xi^{(\Lambda)} \approx 2U_\Lambda^{(\Lambda)}.
 \tag{24}$$

which together with the estimated value of hyperon potential depths in hyperon matter provides effective constraints on scalar coupling constants to the σ^* meson. The currently obtained value of the $U_\Lambda^{(\Lambda)}$ potential at the level of 5 MeV permits the existence of additional parameter set which reproduces this weaker $\Lambda\Lambda$ interaction. In the text this parameter set is marked as weak, whereas strong denotes the stronger $\Lambda\Lambda$ interaction for $U_\Lambda^{(\Lambda)} \simeq 20$ MeV. The relation 24 indicates that for the weak $\Lambda\Lambda$ interaction the potential $U_\Xi^{(\Xi)}$ takes the value $\simeq 10$ MeV whereas for the strong interaction $U_\Xi^{(\Xi)} \simeq 40$ MeV. The vector coupling constants for hyperons are determined from $SU(6)$ symmetry [27] as

$$\frac{1}{2}g_{\omega\Lambda} = \frac{1}{2}g_{\omega\Sigma} = g_{\omega\Xi} = \frac{1}{3}g_{\omega N}
 \tag{25}$$

$$\begin{aligned}\frac{1}{2}g_{\rho\Sigma} &= g_{\rho\Xi} = g_{\rho N}; g_{\rho\Lambda} = 0 \\ 2g_{\phi\Lambda} &= 2g_{\phi\Sigma} = g_{\phi\Xi} = \frac{2\sqrt{2}}{3}g_{\omega N}.\end{aligned}$$

5. Infinite symmetric strange hadronic matter.

For the symmetric strange hadronic matter there no isospin dependence, and there is no contribution coming from the ρ meson field. There are only two conserved charges: the baryon number $n_b = n_\Lambda + n_N + n_\Xi$ and the strangeness number $n_s = n_\Lambda + 2n_\Xi$. These two conserved charges allow one to define the parameter which specifies the strangeness contents in the system and is strictly connected to the appearance of particular hyperon species in the model

$$f_s = \frac{n_s}{n_b} = \frac{n_\Lambda + 2n_\Xi}{n_b}. \quad (26)$$

In a multi-strange system, for sufficient number density of Λ hyperons, the process $\Lambda + \Lambda \rightarrow \Xi + N$, where N stands for nucleon, becomes energetically allowed. Thus, beside N and Λ also Ξ^- and Ξ^0 hyperons have to contribute to the composition of strange hadronic matter. In general the chemical equilibrium conditions for the processes $\Lambda + \Lambda \rightarrow n + \Xi^0$ and $\Lambda + \Lambda \rightarrow p + \Xi^-$ are established by the following relations between chemical potentials

$$2\mu_\Lambda = \mu_n + \mu_{\Xi^0} \quad 2\mu_\Lambda = \mu_p + \mu_{\Xi^-}. \quad (27)$$

This relation for symmetric matter can be rewritten as $2\mu_\Lambda = \mu_N + \mu_\Xi$. The chemical potential μ_B ($B = N, \Lambda, \Xi$) through the Hugenholtz-van-Hove theorem is related to the Fermi energy of each baryon in the following way

$$\mu_B = \sqrt{m_{B,eff}^2 + k_{F,B}^2} + g_{\omega B}w_0 + g_{\phi B}f_0. \quad (28)$$

The binding energy of the system can be obtained from the following relation

$$Eb = \frac{1}{n_b}(\varepsilon - Y_N m_N - Y_\Lambda m_\Lambda - Y_\Xi m_\Xi) \quad (29)$$

where Y_B ($B = N, \Lambda, \Xi$) denotes concentrations of particular baryons.

6. Results

The density dependence of binding energies of multi-strange system involving nucleons, Λ and Ξ hyperons for different parameter sets are presented in Fig.1 and Fig.2. For each parameterization two separated cases are considered, namely the strong and weak $Y - Y$ interactions. Individual lines represent binding energies obtained for different values of strangeness fraction f_s . In all cases the value $f_s = 0$ corresponds to the state when only nucleons are present in the system and the equation of state characteristic to nuclear matter is reproduced. The equilibrium density n_{b_0} can be obtained by minimizing the binding energy with respect to the baryon number density n_B . Increasing the value

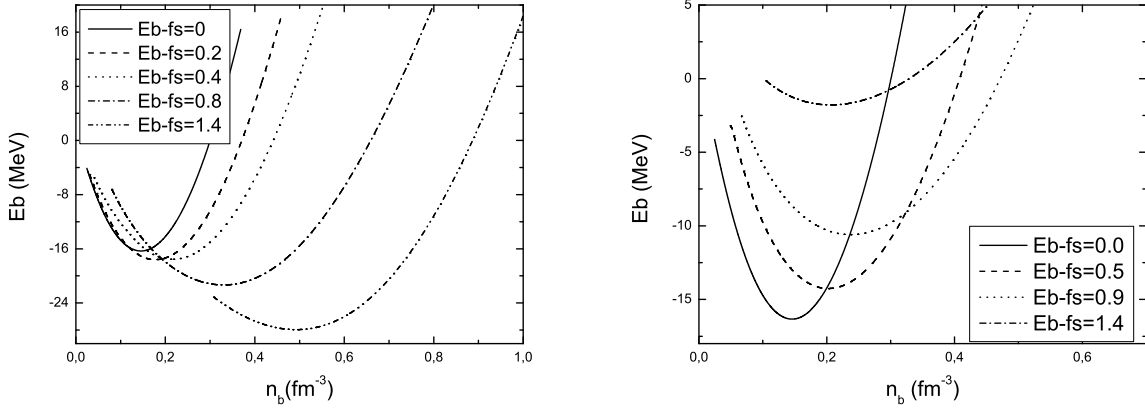


Figure 1. Density dependence of the binding energy Eb for the TM1 parameter set obtained for different values of strangeness fraction fs . The left panel presents results for the strong and the right panel for the weak $Y - Y$ interaction models.

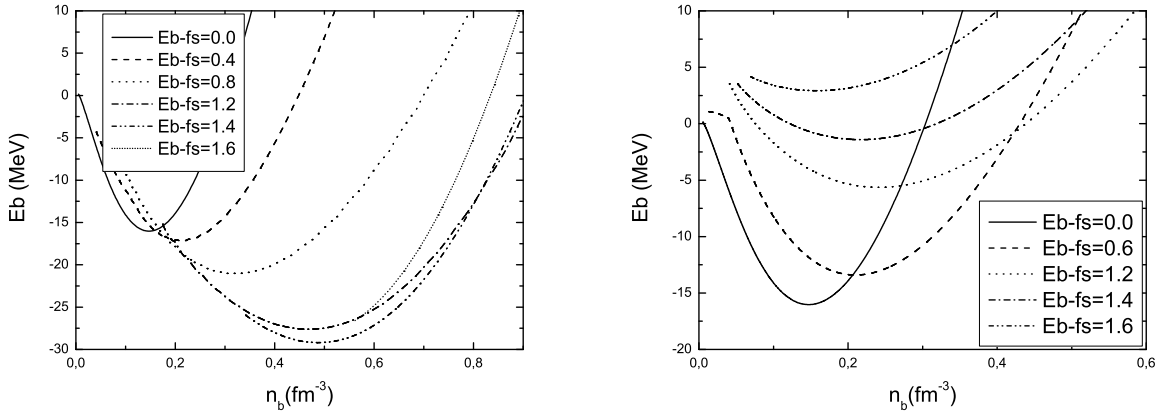


Figure 2. Density dependence of the binding energy Eb for the TMA parameter set obtained for different values of strangeness contents fs . The left panel presents results for the strong $Y - Y$ interaction, the right panel for the weak interaction model.

of the parameter f_s , what is equivalent with the increasing value of the strangeness contents in the matter, the binding energy for each fixed value of the parameter fs has been calculated. The minimum values of binding energies for the fixed values of fs have been determined and the results are plotted in Fig.3. For both parameterizations (TM1 and TMA), in the case of strong $Y - Y$ interaction the increasing value of fs leads to more bound system with the minimum shifted towards higher densities. Contrary to this situation the increasing value of strangeness contents in hyperon matter

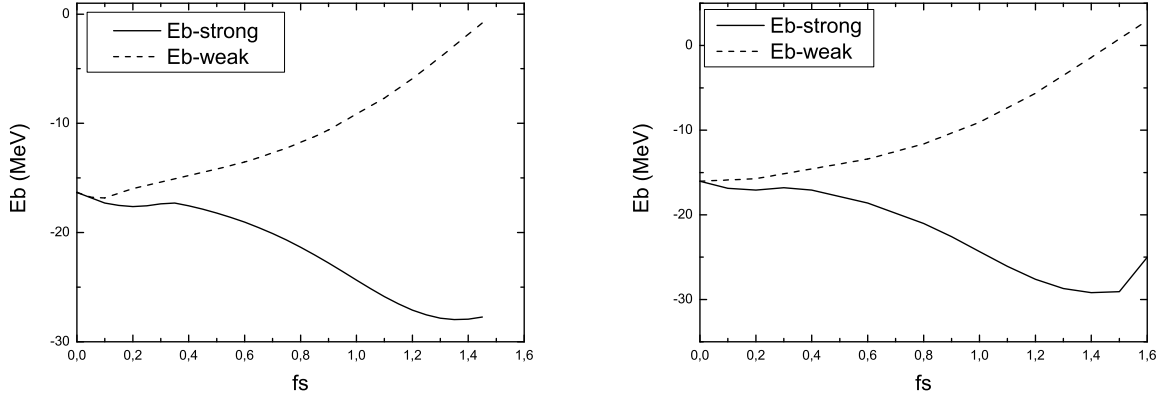


Figure 3. The minimized energy per baryon for the TM1(left panel) and TMA (right panel) parameter sets calculated for the strong and weak $Y - Y$ interaction models.

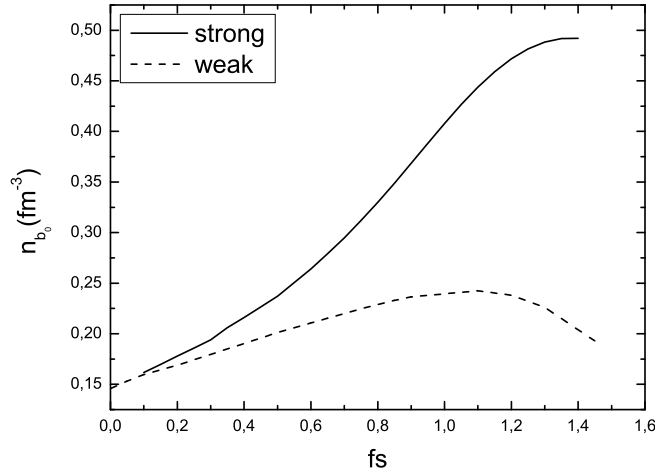


Figure 4. The equilibrium density n_{b_0} as a function of strangeness contents fs .

characterized by weak $Y - Y$ interaction gives shallower minima in the result. In Fig 4 the equilibrium density n_{b_0} as a function of strangeness contents for the two cases mentioned above is presented. The results are depicted for the TM1 parametrization. Relative concentrations of Λ and Ξ hyperons in the case of symmetric strange hadronic matter are presented in Fig.5. In both cases the onset of Λ hyperon is followed by the onset of Ξ hyperon. The populations of Λ hyperons obtained in the TM1 and TMA-weak models are reduced in comparison with those calculated for the strong $Y - Y$ interaction models. Concentrations of Ξ hyperons are higher for the weak TM1 and TMA models. In the case of weak $Y - Y$ interaction model the Ξ hyperon thresholds

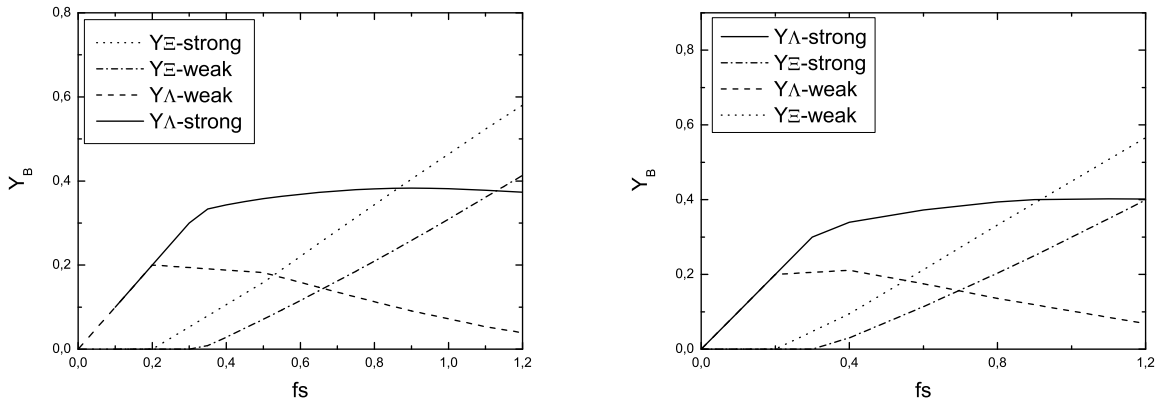


Figure 5. Relative concentrations of Λ and Ξ hyperons in strange hyperon matter for the TM1 (left panel) and TMA (right panel) parameter sets.

are shifted towards lower strangeness fractions. This has an influence on the properties of neutron star matter.

7. Hyperon star matter.

Neutron star interiors and relativistic heavy ion collisions offer suitable environment for the existence of multi-strange hyperon system. In the case of relativistic heavy ion collisions hot and dense nuclear matter is probed whereas neutron star interiors represent the density dominated scenario ($T \sim 0$). The analysis of the role of strangeness in nuclear structure in the aspect of multi-strange system is of great importance for neutron star matter. An imperfect knowledge of the neutron star matter equation of state, especially in the presence of hyperons, causes many uncertainties in determining neutron star structure. It seems to be very important to estimate the influence of nucleon-hyperon and hyperon-hyperon interaction on the equation of state. The comparison between weak interaction time scales (10^{-10} s) and a time scale connected with the lifetime of a relevant star indicates that there is a difference between the neutron star matter constrained by charge neutrality and generalized β equilibrium and the matter in high energy collisions; the latter matter is constrained by isospin symmetry and strangeness conservation. The condition of β equilibrium in the case of neutron star matter implies the presence of leptons and is realized by adding electrons and muons to the baryonic matter. The Lagrangian of free leptons has the following form (30)

$$L_l = \sum_{L=e,\mu} \bar{\psi}_L (i\gamma^\mu \partial_\mu - m_L) \psi_L. \quad (30)$$

In general, in neutron star matter muons start to appear after μ_e has reached the value equal to the muon mass. The appearance of muons not only reduces the number of

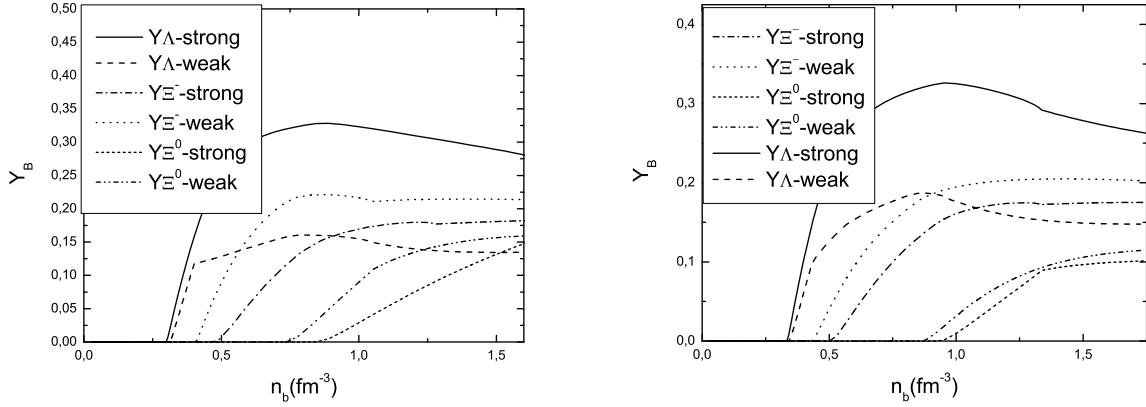


Figure 6. Relative concentrations of hyperons in hyperon star matter as a function of baryon number density for the TM1 model (left panel) and TMA model (right panel).

electrons but also affects the proton fraction. The requirements of charge neutrality

$$n_p = n_e + n_\mu + n_{\Xi^-} \quad (31)$$

and equilibrium under the weak processes

$$B_1 \rightarrow B_2 + L \quad B_2 + L \rightarrow B_1 \quad (32)$$

(B_1 and B_2 denote baryons) is decisive in determining the composition of the hyperon star matter. The equilibrium conditions between baryonic and leptonic species, which are present in hyperon star matter, lead to the following relations between their chemical potentials

$$\begin{aligned} \mu_p &= \mu_n - \mu_e & \mu_\Lambda &= \mu_{\Xi^0} = \mu_n \\ \mu_{\Xi^-} &= \mu_n + \mu_e & \mu_\mu &= \mu_e. \end{aligned} \quad (33)$$

The relations which determine the chemical potentials (28) and effective baryon masses (20) indicate that the composition of hyperon star matter is altered when the strength of the hyperon-hyperon interaction is changed. Fig.6 presents fractions of particular strange baryon species Y_B as a function of baryon number density n_B for TM1 and TMA parameterizations. Starting the analysis of these graphs from moderate densities it is evident that Λ hyperons are the most abundant strange baryons. Λ is also the first strange baryon that emerges in hyperon star matter, it is followed by Ξ^- and Ξ^0 hyperons. For the weak and strong $Y-Y$ interaction models the sequence of appearance of hyperons is the same however, in the case of the weak $Y-Y$ interaction the threshold for the Ξ^- and Ξ^0 hyperons are shifted towards lower densities. Due to the repulsive potential of Σ hyperons their onset points are possible at very high densities which are not relevant for neutron stars. In the case of weak $Y-Y$ interaction the population of Λ hyperons is reduced whereas relative concentrations of Ξ^- and Ξ^0 hyperons are

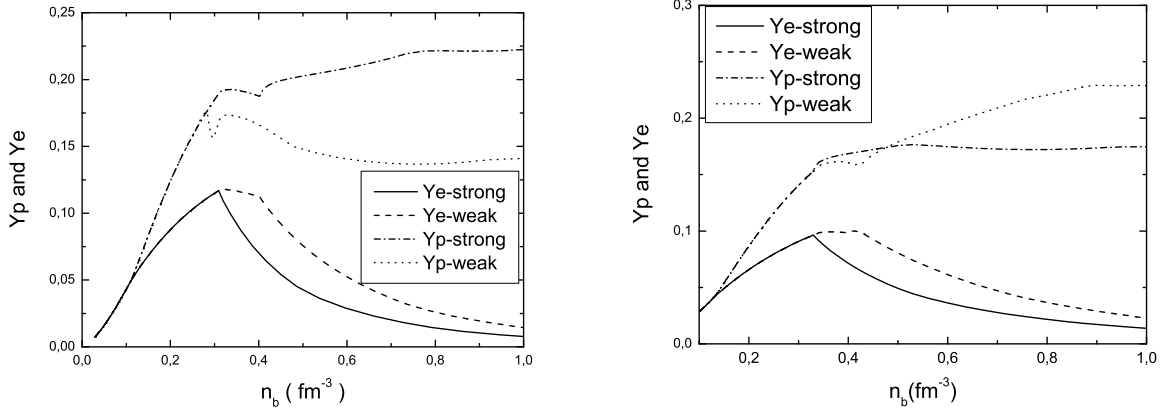


Figure 7. Concentrations of protons and electrons in hyperon star matter as a function of baryon number density for the TM1 model (left panel) and TMA model (right panel).

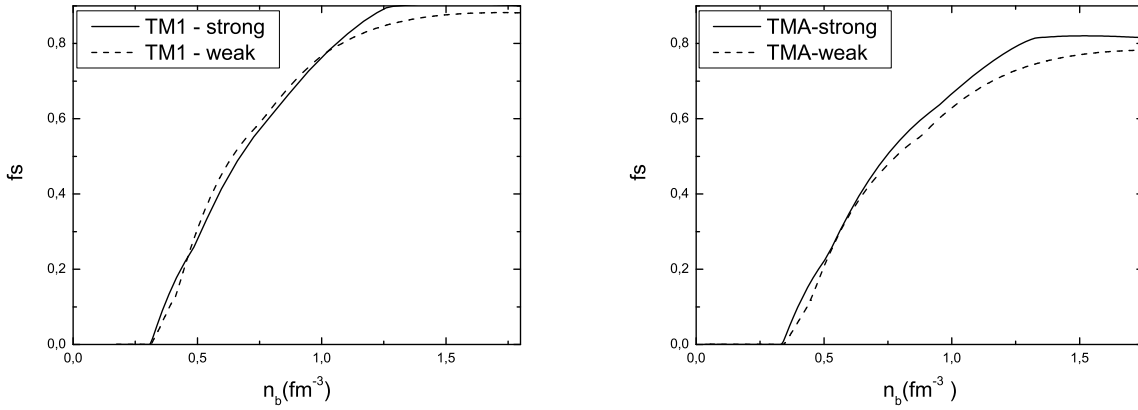


Figure 8. The strangeness contents as a function of baryon number density for the TM1 model (left panel) and TMA model (right panel).

enhanced.

The populations of protons and leptons are also altered by the change of the strength of hyperon coupling constants. Through the requirement of charge neutrality and β -equilibrium condition the onset points and concentrations of hyperons affect the negatively charged lepton and proton abundance. Populations of protons for TM1 and TMA parameterizations increase for the weak $Y - Y$ interaction models. Results are presented in Fig.7. The hyperonization of matter in the presented models can be also analyzed through the density dependence of the strangeness fraction. The density dependence of the fs parameter in the hyperon star matter is depicted in Fig.8. For

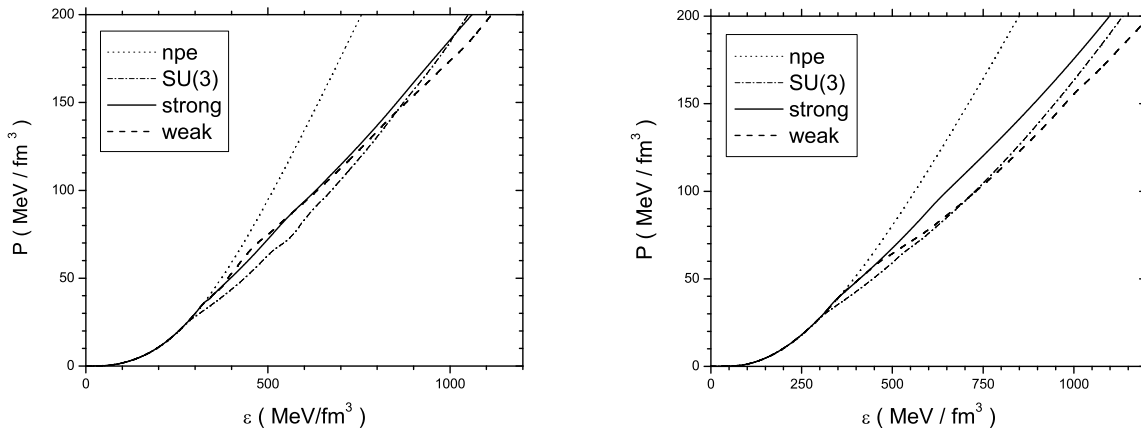


Figure 9. Equation of state for the TM1 (left panel) and TMA models (right panel).

the TMA parameter set more hyperon rich matter is obtained for the strong $Y - Y$ interaction model, the TM1 parameter set gives the same result for very high densities, for moderate densities the strangeness contents is higher for the weak model.

The equation of state of the system can be calculated from the stress-energy density tensor $T_{\mu\nu}$ which is defined as

$$T_{\mu\nu} = \sum_a \partial_\nu \Phi^a(x) \frac{\partial L(x)}{\partial(\partial^\mu \Phi^a(x))} - g_{\mu\nu} L(x) \quad (34)$$

where $\Phi^a = (\phi_M, \psi_B, \psi_L)$ and $\phi_M = (\sigma, \omega, \rho, \sigma^*, \phi)$. The equation of state also has been constructed for the strong and weak $Y - Y$ interactions, for the chosen TM1 and TMA parameterizations. The results are presented in Fig.9 where besides the equations of state obtained for the parameterizations discussed in this paper two other selected equations of state are shown. The first represents the neutron star model (with zero strangeness) and the second the hyperon star model with hyperon couplings derived from the quark model [26]. Generally the equation of state obtained for the weak $Y - Y$ interaction model is less stiff than for the strong model. However, there is an energy density range for which the weak model gives the stiffer equation of state than the strong $Y - Y$ interaction model. The obtained form of the equation of state is influenced by considerably altered effective baryon masses. The results are presented in Fig. 10. On specifying the equation of state the properties and structure of neutron stars can be obtained from hydrostatic equilibrium equations of Tolman, Oppenheimer and Volkoff. The application of the composite equation of state constructed by adding Bonn and Negele-Vauterin equations of state allows us to calculate the neutron star structure for the entire neutron star density span. At higher densities the equation of state depends on the nature of strong interactions hence the strength of hyperon-hyperon interactions should exert influence on neutron star parameters. The calculated mass-radius relations

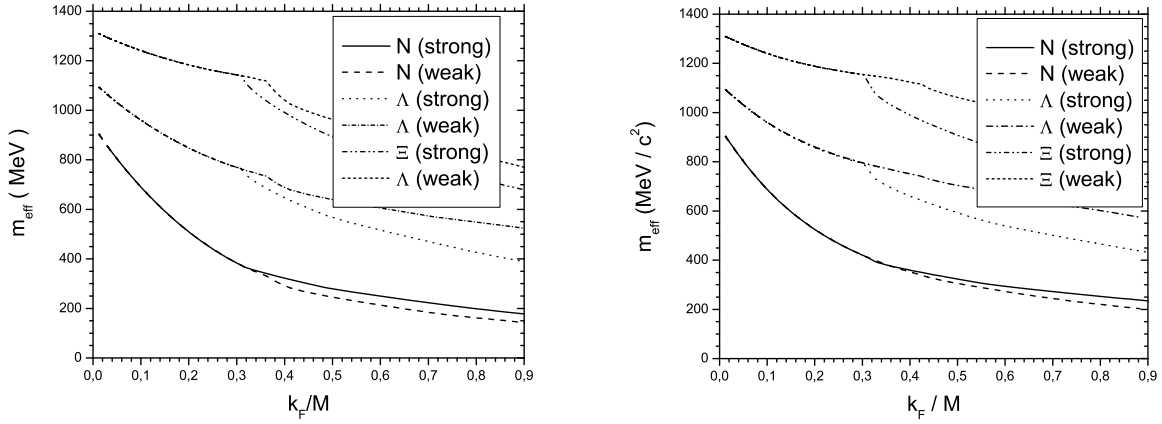


Figure 10. Density dependance of the effective baryon masses for the TM1 (left panel) and TMA models (right panel).

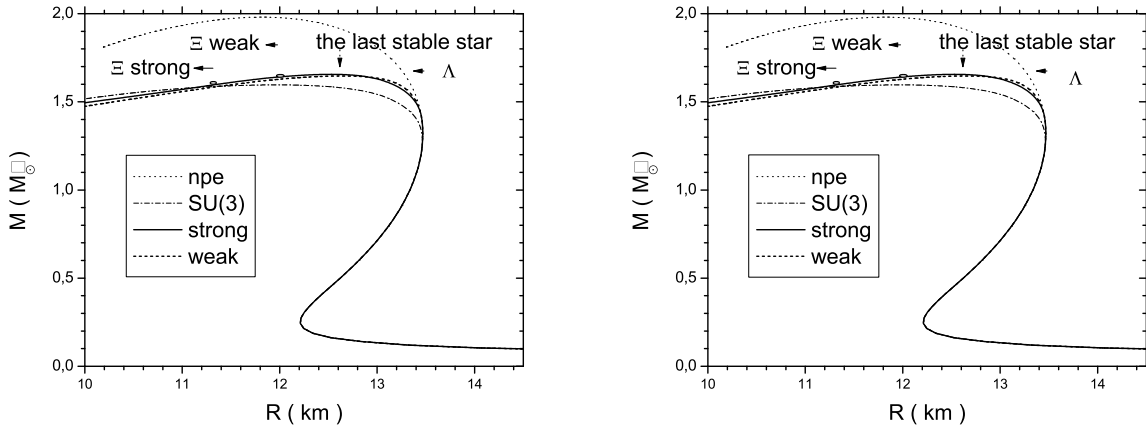


Figure 11. The mass radius relation for the TM1 (left panel) and TMA models (right panel). Dots represent the configurations in which Ξ hyperons appear.

for the determined forms of the equations of state are presented in Fig.11. In Table 4 the parameters of the maximum mass configurations are collected. From Fig.6 it is evident that Ξ^- and Ξ^0 hyperons emerge at very high densities. Although their onset points in the case of weak $Y - Y$ interaction models are shifted towards lower densities, still their presence in stable neutron star configuration is uncertain. In Table 5 the star parameters for the appearance of Ξ hyperons are collected. The value of densities, masses and radii collected in the Table 5 indicate that Ξ hyperons do not appear in stable hyperon star configurations for both parameter sets. Thus only Λ hyperon will

		$\rho_c [g/cm^3]$	R [km]	$M_{max} [M_\odot]$
TM1	weak	6.16×10^{14}	12.88	1.82
	strong	6.60×10^{14}	12.65	1.80
TMA	weak	6.04×10^{14}	12.64	1.64
	strong	6.28×10^{14}	12.53	1.66

Table 4. Neutron star parameters for the maximum mass configurations.

		$\rho_x [g/cm^3]$	R [km]	$M [M_\odot]$
TM1	weak	7.62×10^{14}	12.55	1.81
	strong	9.40×10^{14}	11.99	1.78
TMA	weak	8.08×10^{14}	12.07	1.63
	strong	9.79×10^{14}	11.67	1.62

Table 5. Neutron star parameters for the appearance of Ξ hyperons.

be present in the composition of hyperon star matter for the considered models. Fig.11 shows the position of the configurations, which parameters are presented in Table 5, on the mass-radius relations.

Neutron stars are purely gravitationally bound compact stars. The gravitational binding energy of a relativistic star is defined as a difference between its gravitational and baryon mass.

$$Eb_g = (M_p - m(R))c^2 \quad (35)$$

where

$$M_p = 4\pi \int_0^R dr r^2 \left(1 - \frac{2Gm(r)}{c^2 r}\right)^{-\frac{1}{2}} \rho(r) \quad (36)$$

Of considerable relevance is the numerical solution of the above equation for the selected equations of state. Fig. 12 depicts the gravitational mass which includes interactions versus the baryonic mass for all the considered models.

8. Conclusions.

The main goal of this paper was to study the influence of the strength of hyperon-hyperon interactions on the properties of the hyperon star matter and on a hyperon star structure. It has been shown that replacing the strong $Y - Y$ interaction model by the weak one introduces large differences in the composition of a hyperon star matter both in the strange and non-strange sectors. There is a considerable reduction of Λ hyperon concentration whereas the concentrations of Ξ^- and Ξ^0 hyperons are enhanced. In the non-strange sector the populations of protons and electrons are changed. The weak model permits larger fractions of protons and electrons. The presence of hyperons in general leads to the softening of the equation of state. For the employed weak $Y - Y$

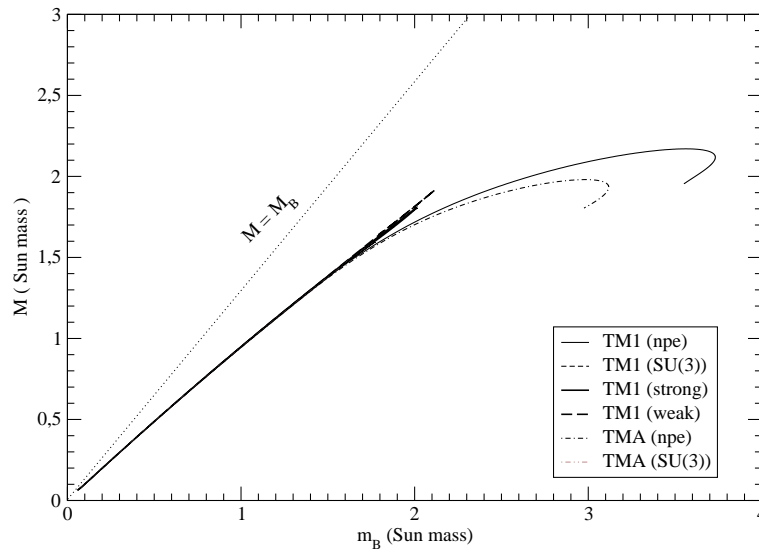


Figure 12. The mass - baryon mass relation.

interaction model there is a density range for which the obtained equation of state is stiffer than the one calculated with the use of the strong model. This is clearly visible in the case of TM1 parameter set. For higher densities the weak model gives less stiff equation of state. The behavior of the equation of state is directly connected with the value of the maximum star mass. Equilibrium conditions namely charge neutrality and β -equilibrium determine the composition of the star. For both parameterizations the onset points for Ξ^- and Ξ^0 hyperons are localized at high densities which are relevant to unstable branches of the mass-radius relations. Thus the obtained stable hyperon star model is composed of neutrons, protons, Λ hyperons and leptons. The appearance of Ξ^- and Ξ^0 hyperons in neutron star interior will be possible in a very special configuration. A protoneutron star model with very high central density can lead to a hyperon star with Ξ and Λ hyperons in its interior. The possibility of the existence of such protoneutron star model will be the subject of future investigations. One can compare the obtained results with those presented in the paper by Schaffner et al. [28], where the analysis of the existence of the third family of stable compact stars has been performed for highly attractive hyperon-hyperon interaction. However, recent experimental data indicate for much weaker strength of $Y - Y$ interaction. Employing these data and the estimated value of the Λ well depth $U_{\Lambda\Lambda} \simeq 5$ MeV the result of the paper [28] can not be confirmed.

References

- [1] Glendenning N.K. 1985 *Astrophys.J.* **293** 470; Also see in *Compact Stars* by N. K Glendenning Springer-Verlag, New York 1997
- [2] Bednarek I., Manka R. 2001 *Int.Journal Mod.Phys.* **D10** 607
- [3] Weber F. *Pulsars as Astrophysical Laboratories for Nuclear and Particle Physics*, IOP Publishing, Philadelphia 1999
- [4] Schaffner-Bielich J., Gal A. 1999 *Phys. Rev.* **C62** 034311

- [5] Serot B.D., Walecka J.D. 1986 *Adv.Nucl.Phys.* **16** 1
- [6] ———1997 *Int.J.Mod.Phys* **E6** 51
- [7] Boguta J. and Bodmer A.R. 1977 *Nucl. Phys.* **A292** 413 *Int. J. Mod. Phys.* **E6** 515
- [8] Bodmer A.R. 1991 *Nucl. Phys.* **A526** 703
- [9] Schaffner J. Dover C.B., Gal A., Greiner C., Millner D.J., Stocker H. 1994 *Ann.Phys.* **235** 35
- [10] Takahashi *et al.* *Phys.Rev.Lett.* 2001 **87** 212502
- [11] Song H.Q., Su R.K., Ku D.H., Qian W.L. 2003 *Phys.Rev.* **C68** 055201
- [12] Prowse D.J. *Phys.Rev.Lett.* 1966 **17** 782
- [13] Dalitz R.H., Davis D.H., Fowler P.H., Motwill A., Pniewski J., Zakrzewski J.A. 1989 *Proc.R. Soc. London* **A 426** 1
- [14] Danysz M. *et al.* 1963 *Nucl.Phys.* **49** 121
- [15] Aoki S.*et al.* 1991 *Prog.Theor.Phys.* **85** 1287
- [16] Dover C.B., Millner D.J., Gal A., Davis D.H. 1991 *Phys.Rev.* **C44**
- [17] Sugahara Y. and Toki H. 1994 *Prog. Theo. Phys* **92** 803
- [18] Yadav A.L., Kaushik M., Toki H. 2004 *Int.J.Mod.Phys.* **13** 647
- [19] Millener D.J., Dover C.B., Gal A. 1988 *Phys.Rev.* **C38** 2700
- [20] Mareš J., Friedman E., Gal A., Jennings B.K. 1905 *Nucl. Phys.* **A594** 311
- [21] Batty C.J., Friedman E., Gal A., Jennings B.K. 1994 *Phys.Lett.* **335** 273
- [22] Balberg S., Gal A., Schaffner J. 1994 *Prog. Theor. Phys. Suppl.* **117**, 325
- [23] Stoks V.G.J., Lee T.S.H., 1999 *Phys. Rev.* **C 60** 024006
- [24] Dover C.B., Gal A. 1983 *Ann.Phys.* **146** 209
- [25] ———1994 *Prog. Theo. Phys.Suppl.* **117** 145
- [26] Ma Z.Y., Toki H., Chen B. Q. and Van Giai N. 1997 *Prog.Theor. Phys.* **98** 917
- [27] Shen H. 2002 *Phys. Rev.***C65** 035802
- [28] Schaffner-Bielich J., Hanauske M., Stöcker H., Greiner W. 2002 *Phys.Rev.Lett.* **89** 171101